



Microwave-Assisted Synthesis and Antibacterial–Anticancer Evaluation of Sulfadiazine-Imine Derivatives

Dhamer Ismael Madab^{1*}, Mohammad M. Al-Tufah², Diaan M. Najim³

^{1,2,3} Directorate of Education, Ministry of Education, Tikrit, Iraq

Email: dhammer.84@gmail.com¹, Mohamadmd282@gmail.com², diaa1988mahmoud@gmail.com³

*Corresponding Author: dhammer.84@gmail.com

Abstract. This study synthesized novel sulfadiazine-imine derivatives (A1 and A2) using a microwave-assisted method by reacting sulfadiazine with orsellinaldehyde and 2-hydroxy-5-methylbenzaldehyde. The synthesis involved the nucleophilic addition of sulfadiazine to the aldehyde groups, forming imine bonds efficiently under microwave irradiation within 15 minutes. The antibacterial efficacy of the synthesized derivatives was tested against *Bacillus subtilis*, *Streptococcus pneumoniae*, and *Escherichia coli* using agar well diffusion methods. The derivatives A1 and A2 exhibited significantly improved antibacterial activities compared to sulfadiazine, with A1 showing the highest efficacy. Specifically, inhibition zones for *Bacillus subtilis* reached 26 mm (A1 at 100 mg/mL) compared to 20 mm for sulfadiazine, and similar trends were observed against *E. coli* and *S. pneumoniae*. Furthermore, the cytotoxic activity against MCF-7 breast cancer cells revealed that both derivatives demonstrated dose-dependent cytotoxicity. For derivative A1, cell viability decreased to 19% at 320 ppm with an estimated IC₅₀ between 40 and 80 ppm. Derivative A2 showed comparable cytotoxic behavior, with cell viability dropping to 12.6% at the highest concentration tested. The enhanced antibacterial and anticancer properties are attributed to increased lipophilicity and improved cellular penetration conferred by the imine functional group. This research highlights the potential of microwave-assisted derivatization of sulfadiazine to produce compounds with promising therapeutic applications.

Keywords: Antibiotics, Antibacterial activity, Anticancer activity, Cytotoxicity, Microwave synthesis.

1. INTRODUCTION

Modern medicine has grown dependent on antibiotics to fight bacterial illnesses that have killed millions. Since their discovery, antibiotics have greatly enhanced life expectancy and surgical success (1). Antibiotic research and refining are necessary to combat infectious illnesses. Antibiotics are essential to medical practice because even minor illnesses might become life-threatening without them (2).

Sulfonamides, such as sulfadiazine, were among the first antibiotics. Sulfadiazine, a synthetic antibiotic from sulfanilamide (3), inhibits bacterial growth by interfering with folic acid production and is frequently used. Sulfadiazine may cure urinary tract infections, meningitis, and pneumonia if appropriately given. Its wide range of action makes restricting or prohibiting alternative treatments worthwhile (4).

Considering sulfadiazine's use outside bacterial illnesses increases its medicinal importance. It is used in therapy combinations for toxoplasmosis, a severe parasitic infection. Silver sulfadiazine also inhibits bacterial colonization and enhances wound healing in burn treatment. Thus, the adaptability of sulfadiazine in systemic and topical therapies highlights its therapeutic value (5).

Researchers have altered sulfadiazine's molecular structure to improve its potency and overcome resistance. Successful adjustments might boost derivative biological activity and pharmacokinetics. Thus, innovative sulfadiazine-based molecules may improve treatment choices and combat antibiotic resistance, making them essential (6).

Due to the growing danger of multidrug-resistant bacteria, studying and optimizing conventional antibiotics like sulfadiazine is crucial. The medical community can better fight infectious illnesses if novel approaches are followed. Understanding sulfadiazine's purpose and how to boost its biological activity is essential to ensure the future success of antimicrobial medicines (7, 8).

This research aims to synthesize novel sulfadiazine-imine derivatives using a microwave-assisted method, characterize these structures by spectroscopy such as FTIR and ¹H-NMR, and evaluate their enhanced antibacterial and anticancer activities compared to the parent compound.

2. MATERIALS AND METHODS

Materials

All chemical materials, such as sulfadiazine, Orsellinaldehyde, and 2-hydroxy-5-methylbenzaldehyde, were obtained from Sigma Aldrich, while the absolute ethanol (99%) was obtained from BDH.

Methodology

Microwave-assisted Sulfadiazine-Imine Synthesis

Dissolve (0.25 g, 1.0 mmol) of sulfadiazine in 15 ml of absolute ethanol. Added (1.0 mole) of corresponding aldehydes, such as orsellinaldehyde and 2-hydroxy-5-methylbenzaldehyde, separately to produce two solutions. The resulting mixtures were refluxed for 15 min in a microwave. The precipitates were synthesized, collected, washed with absolute ethanol several times, dried, and kept (9).

Evaluation of the antibacterial efficacy of sulfadiazine and its imine derivatives (A1 and A2)

Some bacteria, such as *Bacillus subtilis*, *Streptococcus pneumoniae*, and *Escherichia coli*, were cultured on Mueller-Hinton agar plates using sterile loops and streaking procedures. A separate well was formed in the agar media. A 50 to 100 Mg/mL volume of the appropriate dilution of sulfadiazine and imine-sulfadiazine compounds (A1 and A2) was

added to each well, facilitating effective absorption. The container was securely sealed and positioned in an incubator maintained at 37 °C overnight, to evaluate it the following day (10).

Molecules Docking Preparation

The novel azomethine derivative (A) was produced and characterized for use in the molecular docking process. ChemDraw Ultra 12.0 software was used to construct the 3D structures of compound (A), followed by energy minimization. The optimized structures by using the DFT approach, and the synthesized chemical (A) was characterized for use in the molecular docking, werecess. ChemDraw Ultra 12.0 was employed to construct the 3D structures of compound (A), subsequently undergoing energy minimization using the B3LYP/6-31G basis set to ascertain the most stable conformation, which was also utilized for calculating the global reactivity descriptors via Gaussian 09 (11). All calculated vibrational frequencies for the medications have positive values, indicating their stability. The optimized structures were consolidated into a single database using (MOE 2015) to analyze ligand affinity, as shown in Figure 2. Figure 1 illustrates the schematic depiction of the docking technique, drug analysis, and reactivity.

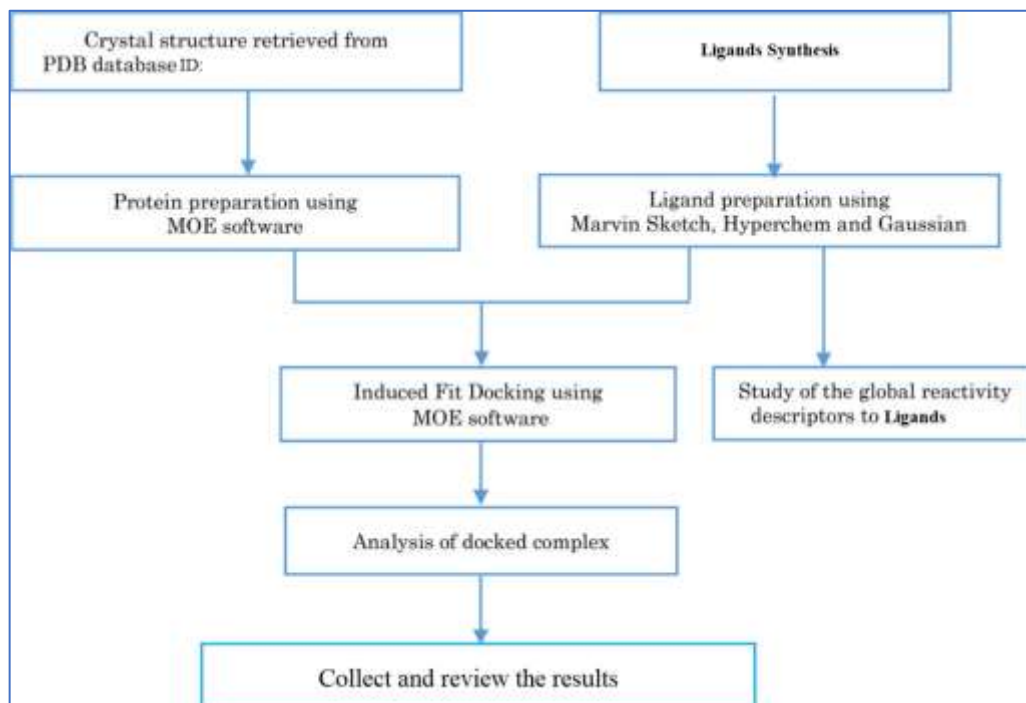


Figure 1: Schematic depiction of the docking process, evaluation of pharmaceuticals, and reactivity.

Receptors preparation

The protein's crystal structure (6ISJ), as shown in Figure 2, was obtained from the Protein Data Bank. The water molecule in the target protein's active site is crucial; thus, it was included in the active site to facilitate the formation of a hydrogen bond between the ligand and the target. Subsequently, the protein structure was refined by rectifying the missing bonds disrupted during X-ray diffraction and incorporating hydrogen atoms. PDB is a reliable repository for the crystal structures of biological macromolecules globally (12).



Figure 2: Crystal structure of the 6ISJ protein.

Ligand-Protein molecular docking

The computations were conducted employed the Molecular Operating Environment (MOE) program. The crystal structures of the protein (6ISJ), as shown in Figure 3 were acquired from the PDK at a resolution of 2.30 Å. A resolution ranging from 1.4 to 2.5 Å is suitable for docking investigations. The optimal RMSD values should approximate 2 Å, with an energy score of -7 kcal/mol or below. These two parameters are often used as benchmarks to assess the validity of the molecular docking results.

3. RESULTS AND DISCUSSION

The microwave-induced nucleophilic addition of sulfadiazine to aldehydes such as orsellinaldehyde and 2-hydroxy-5-methylbenzaldehyde produces imine derivatives quickly and efficiently, as shown in Scheme 1. A transitory carbinolamine intermediate forms when the sulfadiazine's leading amine group's nucleophilic nitrogen atom hits the aldehyde's carbonyl group's electrophilic carbon. The molecular-level heating of polar reactants with microwave aid speeds up molecular collisions and improves reaction kinetics. Since the carbinolamine intermediate quickly dehydrates, it forms a carbon-nitrogen double bond (C=N) like the imine structure (13). The homogeneous and volumetric heating from microwave irradiation promotes bond formation, reduces side reactions, and boosts yield and purity. Hydroxyl groups on aldehydes, notably orsellinaldehyde and 2-hydroxy-5-methylbenzaldehyde, stabilize the intermediate by hydrogen bonding, speeding microwave dehydration. Schiff base production is selective and efficient at moderate microwave power and short irradiation duration. Due to microwaves' efficient energy transfer and localized superheating effects, microwave-assisted synthesis produces sulfadiazine derivatives faster, purer, and with less solvent (14).

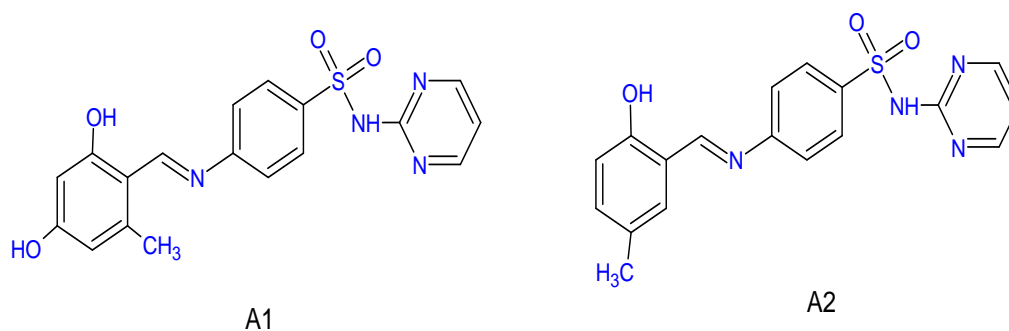


Figure 3: Structures of imine derivatives synthesized A1 and A2.

FTIR (cm^{-1}), the spectrum of derivative A1 showed a broad band of the hydroxyl group at 3400, C-H of aromatic ring at 3035, C-H of aliphatic chain at 2972 and 2867, the azomethine group showed at 1645, and C=C of aromatic ring showed at 1568 (15), as shown in Figure 5.

$^1\text{H-NMR}$ (ppm) that used DMSO- d_6 as solvent: The derivative A1 showed 9.77 for (s, 1H, OH) the proton of the hydroxyl group and 7.26-8.32 for (m, 16H, Ar) protons of aromatic rings, 8.76 for (s, 1H, CH) the proton of the azomethine group, 2.15 for (s, 3H, CH_3) for methyl group (16), as shown in Figure 6.

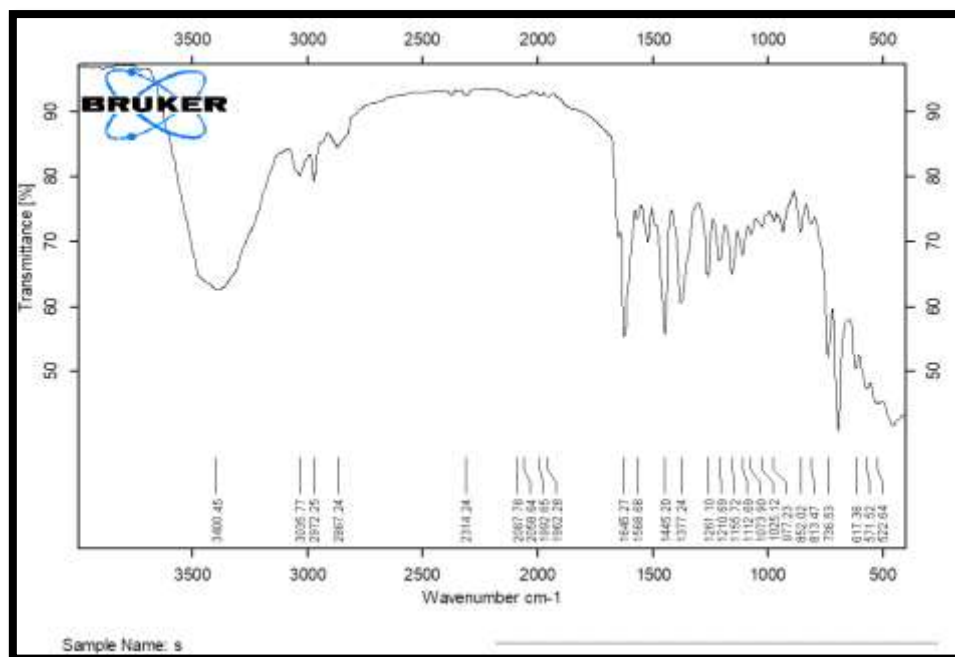


Figure 4: FTIR spectrum of derivative A1.

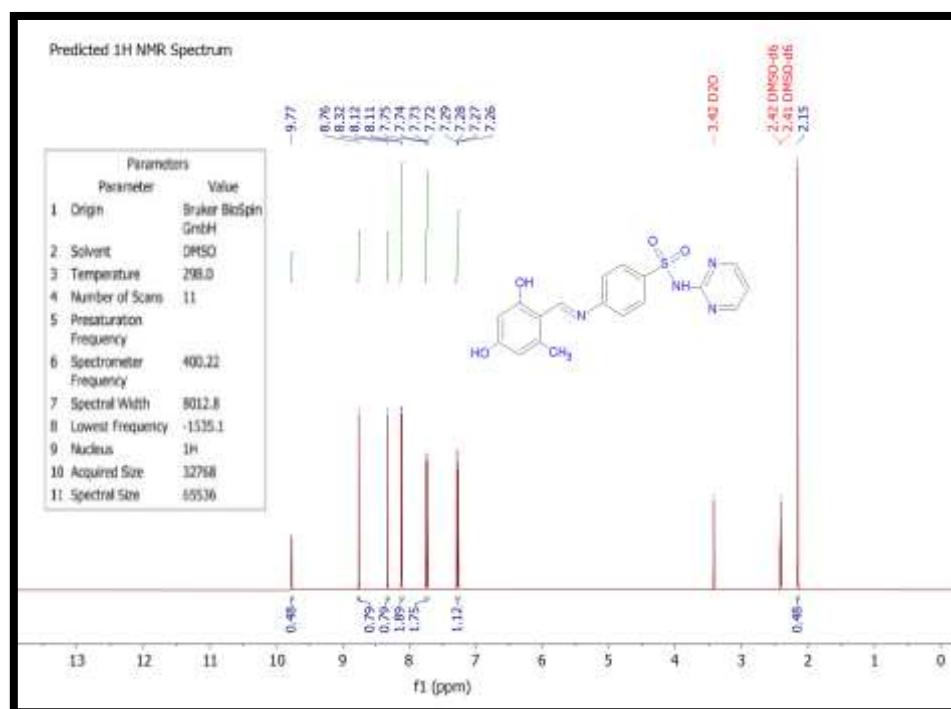


Figure 5: ¹H-NMR spectrum of derivative A1.

FTIR (cm⁻¹): The spectrum of derivative A1 showed a broad band of the hydroxyl group at 3359, C-H of the aliphatic chain at 2981 and 2850, the azomethine group at 1629, and C=C of the aromatic ring at 1593 (17), as shown in Figure 7.

$^1\text{H-NMR}$ (ppm) that used DMSO-d₆ as solvent: The derivative A1 showed 9.59 for (s, 1H, OH) the proton of the hydroxyl group and 7.22-7.83 for (m, 16H, Ar) protons of aromatic rings, 8.68 for (s, 1H, CH) the proton of the azomethine group, 2.10 for (s, 3H, CH₃) for methyl group (16), as shown in Figure 8.

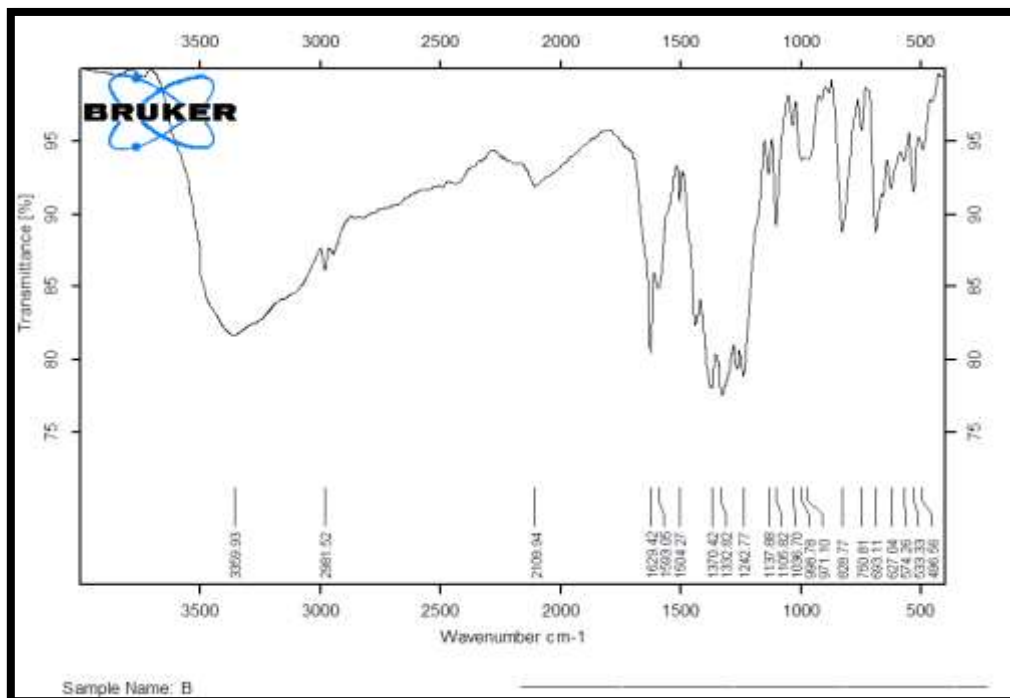


Figure 6: FTIR spectrum of derivative A2.

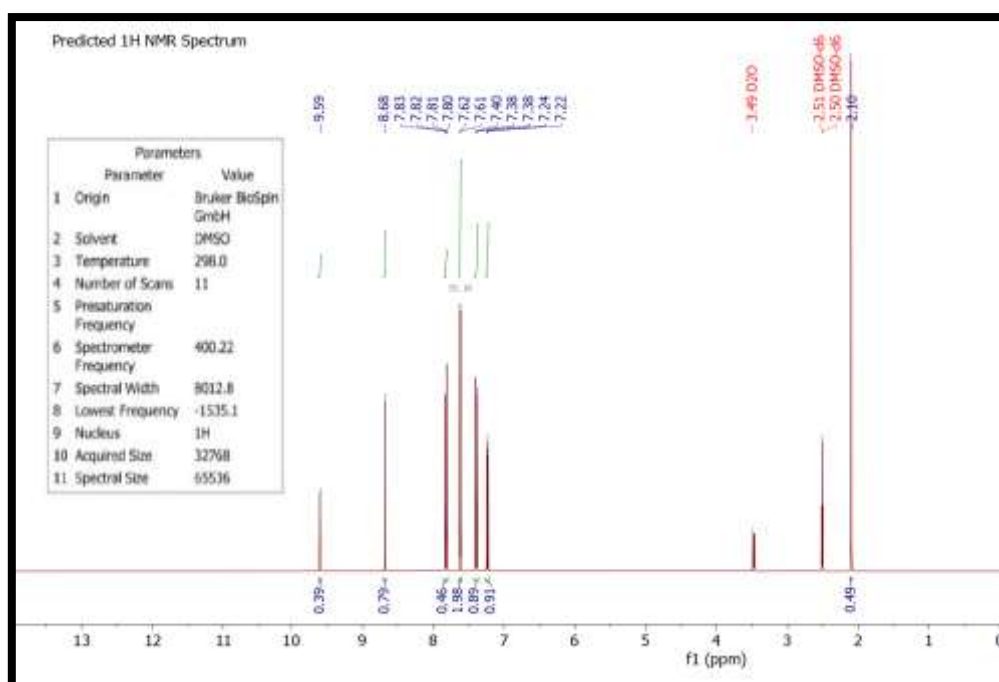


Figure 7: $^1\text{H-NMR}$ spectrum of derivative A2.

Figure 9 illustrates the antibacterial efficacy of sulfadiazine and its imine derivatives (A1 and A2) against *Bacillus subtilis*. Sulfadiazine alone generated inhibitory zones of 16 mm at 50 mg/mL and 20 mm at 100 mg/mL. Both derivatives A1 and A2 demonstrated much wider inhibition zones than the original drug. The derivative A1 had the most significant activity, with inhibition zones of 20 mm and 26 mm at the two respective doses, whilst derivative A2 showed moderate activity with measurements of 17 mm and 22 mm. The data unequivocally demonstrate that the imine alterations enhanced antibacterial efficacy against *Bacillus subtilis*, particularly at elevated doses.

Likewise, Figure 10 displays the antibacterial outcomes against *Escherichia coli*. Sulfadiazine exhibited significant inhibition, with zones of 13 mm at 50 mg/mL and 17 mm at 100 mg/mL. In contrast, the derivative A1 had enhanced antibacterial efficacy, attaining inhibition zones of 15 mm and 20 mm, whilst derivative A2 closely trailed with 14 mm and 18 mm. While the distinctions between sulfadiazine and its derivatives were not as pronounced as in *Bacillus subtilis*, it is clear that chemical alteration marginally improved effectiveness, especially for derivative A1. This indicates that the derivatives may partly surmount the permeability barrier often associated with Gram-negative bacteria such as *E. coli*.

The activity against *Streptococcus pneumoniae* is seen in Figure 11. Sulfadiazine generated inhibition zones of 13 mm and 18 mm, which were relatively mild. The derivative A1 consistently showed superior efficacy among the evaluated drugs, achieving zones of 14 mm at 50 mg/mL and a significant rise to 21 mm at 100 mg/mL. The derivative A2 demonstrated enhanced action compared to sulfadiazine, yielding 13 mm and 19 mm zones. The data indicate that both imine derivatives exhibit more potency than the original medication against *Streptococcus pneumoniae*, with derivative A1 demonstrating the most significant antibacterial action.

Upon comparison of the overall findings across the three bacterial strains, it is clear that the imine derivatives (A1 and A2) consistently surpassed sulfadiazine at both tested doses. The improvement in biological activity may be ascribed to the heightened lipophilicity and enhanced cell membrane penetration provided by the imine functional group. The derivative A1 consistently exhibited larger inhibition zones than derivative A2, indicating that the substituent in derivative A1 enhances antibacterial efficacy. The results suggest that the chemical derivatization of sulfadiazine into imine analogues is an efficient method to improve antibacterial efficacy, especially against Gram-positive and Gram-negative infections.

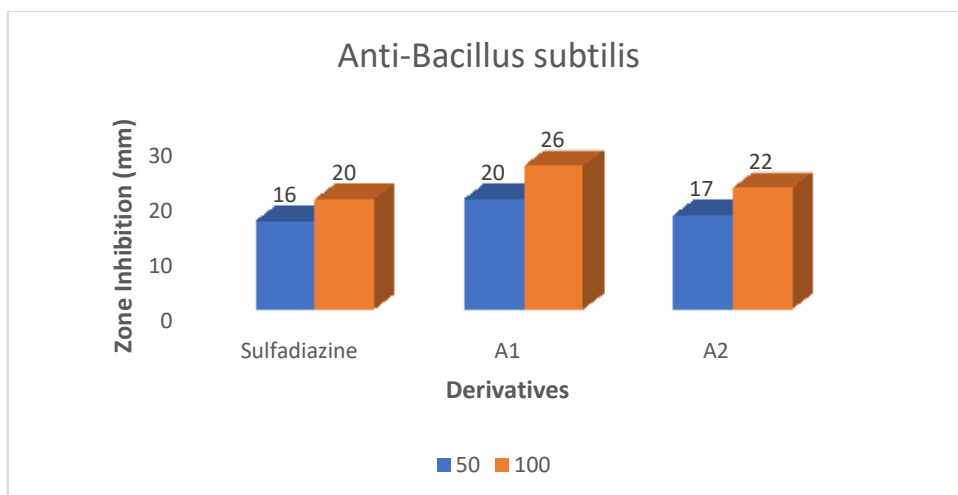


Figure 8: Biological activity of synthesized derivatives against *Bacillus subtilis*.

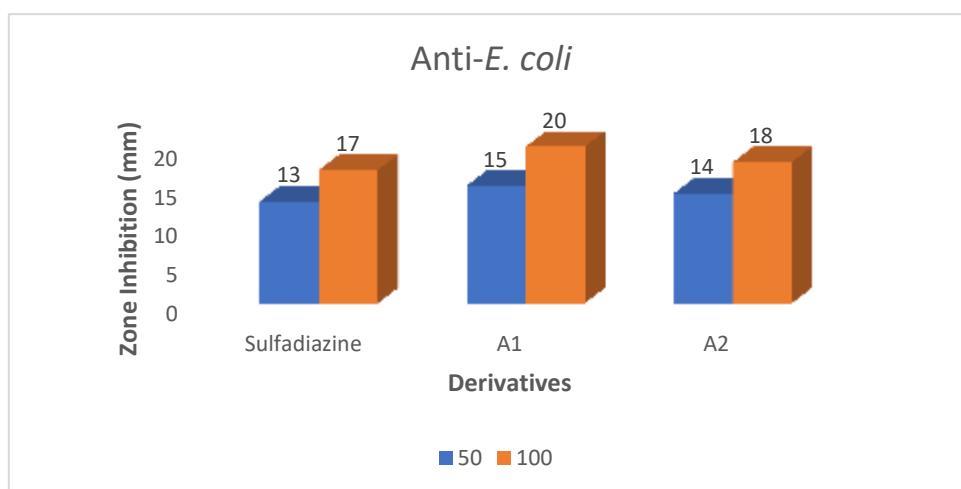


Figure 9: Biological activity of synthesized derivatives against *E. coli*.

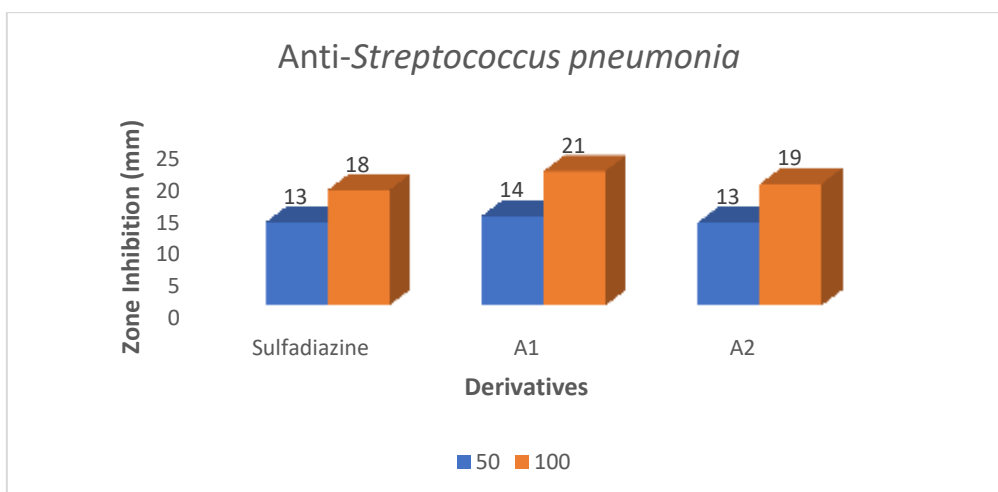


Figure 10: Biological activity of synthesized derivatives against *Streptococcus*.

Figure 11 and Table 1 show the 24-hour cytotoxic activity of the produced sulfadiazine-imine derivative A1 against MCF-7 breast cancer cells. Cell viability decreased gradually from 20 to 320 ppm A1, showing a dose-dependent impact. Viability dropped to 68% at 20 ppm and 19% at 320 ppm. This considerable decrease shows that A1 has anticancer effects. The cytotoxic impact was minimal at 20 ppm, but greater doses, especially over 80 ppm, significantly inhibited cell growth. The cytotoxic effects were reproducible and reliable due to modest standard deviations between duplicates, particularly at mid to high doses. The trend suggests that derivative A1's IC50 value, the concentration needed to block 50% of cell viability, would be between 40 and 80 ppm, demonstrating its potency. Thus, chemical transformation of sulfadiazine into the imine derivative A1 significantly increases its anticancer activity, likely owing to greater cellular target contact or absorption. Further improvements of the A1 structure might boost its anticancer potential.

Figure 14 and Table 1 show the 24-hour cytotoxic effects of the sulfadiazine-imine derivative A2 on MCF-7 breast cancer cells. Cell viability decreased significantly when A2 concentration grew from 20 ppm to 320 ppm, indicating a dose-dependent relationship. Viability remained high at 64% at 20 ppm; however, increasing to 80 ppm significantly lowered viability to 33%. This shows that moderate to high dosages of A2 are more cytotoxic. The data is also reliable since the standard deviations were minimal across concentrations. Also, viability decreased more at doses over 80 ppm than lower ones, suggesting a threshold effect. The chemical structure of A2 likely enhances its anticancer efficacy by improving cellular penetration or interaction with intracellular targets (18). The findings indicate that derivative A2 may be a potential anticancer candidate, especially if structural modifications improve selectivity and potency (19).

Table 1: IC50 rates of derivatives A1 and A2 on MCF-7 cell viability.

Concentration (PPM)	Derivative A1		Derivative A2	
	Mean	SD	Mean	SD
0	100.9808	4.563203	100.624	2.393088
20	68.33967	2.044869	64.365	2.830745
40	56.801	0.809419	49.82233	2.600586
80	43.46229	4.150698	33.37833	1.972511
160	28.59818	1.307276	22.2101	2.781846
320	19.23847	1.446269	12.596	2.123495

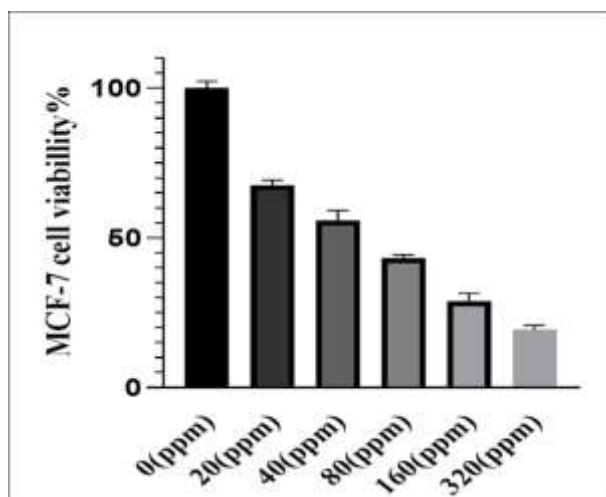


Figure 11. Effect of derivative A1 on MCF-7 cell viability.

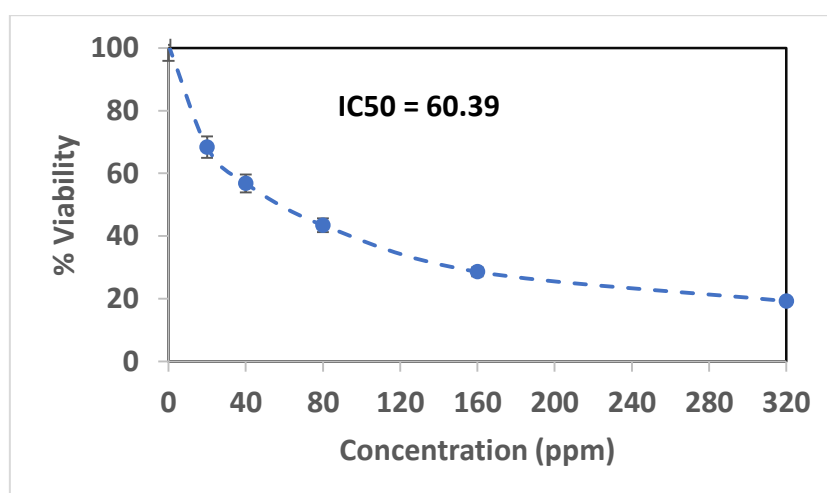


Figure 12: IC₅₀ of derivative A1 on MCF-7 cell viability.

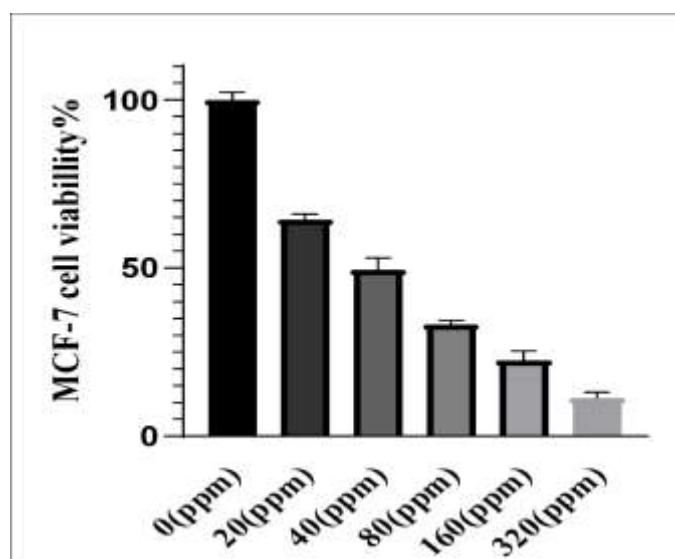


Figure 13. Effect of derivative A2 on MCF-7 cell viability.

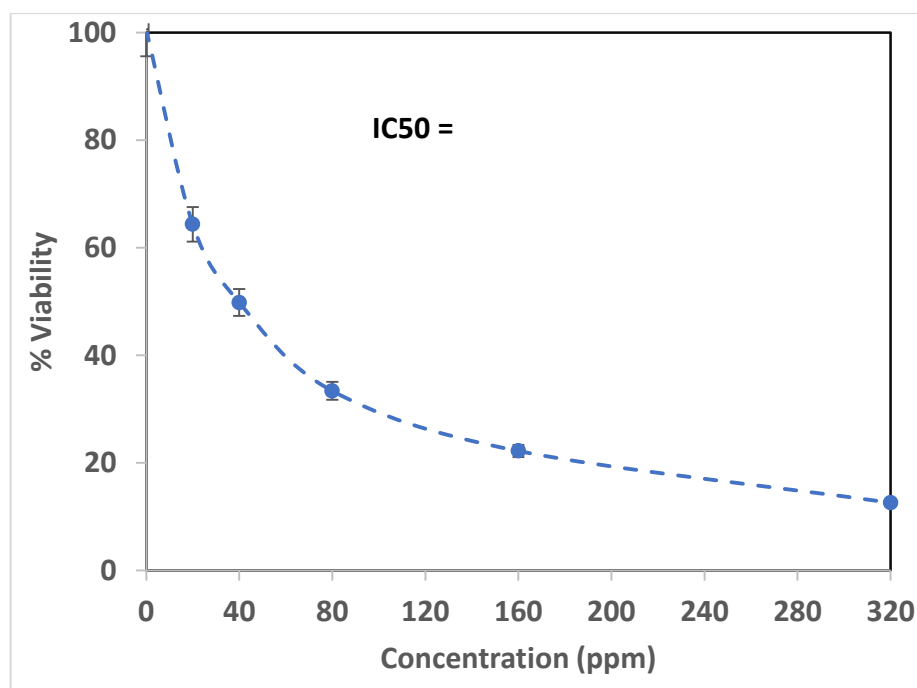


Figure 14. IC50 of derivative A2 on MCF-7 cell viability.

Molecular docking

Molecular docking is used as a fundamental tool in the drug discovery pipeline. In the present study, MOE software was applied to perform all molecular docking calculations and predict the binding modes of the prepared compound (A) with the protein (6ISJ) (Figure 16). The predicted binding affinities and features of the investigated compound (A) towards (6ISJ) are listed in the next tables (20). These tables show the best binding poses of compound (A) against target proteins. The 2D and 3D representations of interactions of the inspected compounds with the key amino acid residues of the (6ISJ) protein are illustrated in the next figures and tables (21). Compound (A) showed good binding affinity values (Table 2 - Table 4) with protein (6ISJ). The binding and mode of interactions of the compound (A) with the (6ISJ) protein are shown in 2D and 3D figures. It has been demonstrated from the interactions that there are primarily different types of interactions (hydrogen bonding and hydrophobic interactions). The results from these figures showed that compound (A) interact with different amino acid residues in three different interactions: H-donor, H-acceptor, and H-pi, as well as two H-acceptor and pi-H interactions with the water and various amino acids. The distance and energy binding of interaction are listed in the next tables.

Table 2: The binding affinity and rmsd result of A compound with 6ISJ.

Compounds/ mseq	Binding Affinity Kcal/mol	Rmsd (Å)	E_score1	E_refine	E_score2
A1/1	-6.75652	1.466182	-12.3211	-31.461	-6.75652
A1/1	-6.74745	0.793563	-13.007	-27.8658	-6.74745
A1/1	-7.15334	1.914486	-12.5199	-26.0692	-7.15334
Standard/std	-7.95335	2.114488	-10.5199	-24.0692	-7.95335

Table 3: Name of compounds and smiles.

Compounds	Binding Affinity Kcal/mol	Rmsd (Å)
A1	-6.75652	1.466182
A1	-6.74745	0.793563
A1	-7.15334	1.914486
standard	-7.95335	2.114488

Table 4: Details of the best pose of protein 6ISJ

Compound s	Binding Affinity Kcal/mo l	Rmsd (Å)	Atom of compoun d	Atom of Recepto r	Involve d receptor residues	Type of interaction bond	Dista nce (Å)	E (kcal/m ol)
A1	- 7.15334	1.9144 86	N 11	SD	MET	(A) H-donor	3.83	-0.4
			N 11	SD	162	(A) H-donor	3.60	-0.7
			O 12	CE	MET	(A) H-	2.85	-1.9
			O 12	CE	162	acceptor	3.13	-1.1
			N 18	CD	LYS 67	(A) H-	3.04	-0.9
				LYS 67	acceptor			
				LYS 67	(A) H-			
standard	- 7.95335	2.1144 88	O25 38	O	HOH	(A) H-	2.58	-2.6
			O24 37	NZ	504	acceptor	2.81	-5.9
			O24 37	NZ	LYS 67	(A) ionic	2.98	-4.6
			O25 38	NZ	LYS 67	(A) ionic	3.90	-0.7
			6-ring	CG1	LYS 67	(A) ionic	4.02	-0.9
			6-ring	CG1	VAL 52	(A) pi-H	3.99	-0.9
					VAL 52	(A) pi-H		

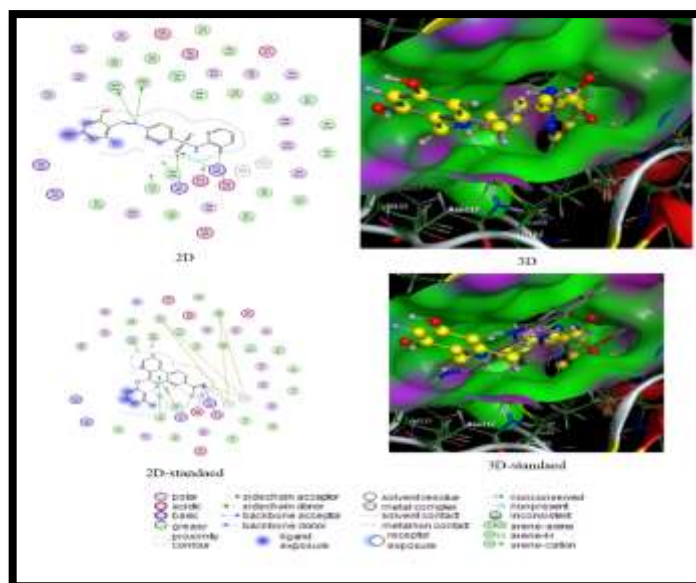


Figure 15: 2D and 3D of the best pose and standard.

In this molecular docking study, compound A1 was evaluated through multiple poses against the 6ISJ protein structure. Among the three docking poses recorded for A1, the one highlighted in green color represents the best result based on its superior binding affinity and RMSD. This specific pose achieved a binding affinity of -7.15334 kcal/mol and an RMSD of 1.914486 Å, values which fall comfortably within the ideal range for stable and effective binding (typically 1.5–2.5 Å). These results indicate that the green-highlighted A1 pose is the most reliable and structurally stable among all the poses tested for this compound.

Energetically, this best A1 pose demonstrated excellent optimization throughout the docking process. It recorded a highly favorable E_{conf} of -135.371, an E_{place} of -92.1969, and an E_{refine} of -26.0692, all indicating that the ligand maintained a low-energy, well-fitted conformation inside the protein’s active site. When compared to the standard compound, which had a slightly better binding affinity of -7.95335 kcal/mol, A1 still performed admirably, especially considering that its RMSD was lower than that of the standard (1.91 Å vs 2.11 Å), suggesting a more consistent binding pose.

Looking at the interaction details, the green-highlighted A1 pose engaged in several meaningful hydrogen bonding interactions, predominantly with the LYS 67 residue and MET 162. Specifically, it formed hydrogen donor interactions with MET 162 (SD) at distances of 3.83 Å and 3.60 Å, and acted as a hydrogen acceptor toward LYS 67 (CE and CD) at distances ranging from 2.85 Å to 3.40 Å. These contacts, while moderate in interaction energy (-0.9 to -1.9 kcal/mol), show that A1 successfully positioned itself to maximize polar interactions critical for binding stability.

In contrast, the standard drug exhibited a broader range of interactions, including strong ionic bonds with LYS 67 and multiple π -H interactions with VAL 52, contributing to its superior binding energy. However, the structural stability advantage shown by the green-highlighted A1 pose (lower RMSD) suggests that while the standard binds slightly stronger energetically, A1 binds more predictably and rigidly, which is highly desirable for drug design.

To conclude, the green-colored pose of A1 emerged as the best configuration in this docking analysis. It demonstrates near-competitive binding energy with the standard, a lower RMSD indicating excellent pose stability, and a focused hydrogen bonding network with critical residues. These attributes make A1, specifically its best pose, a promising scaffold for further development against the 6ISJ protein target.

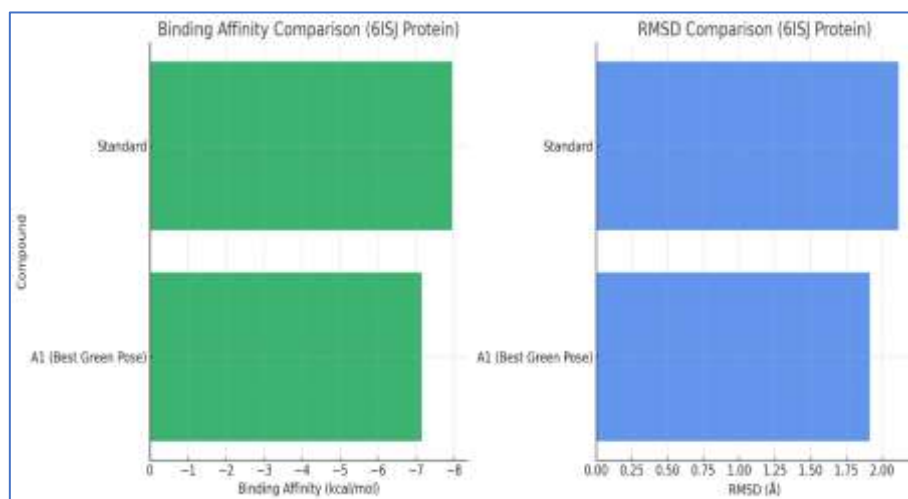


Figure 17: This composite figure compares the docking performance of the green-highlighted pose of compound A1 (“A1 (Best Green Pose)”) with that of the standard drug against the 6ISJ protein.

The left panel displays the binding affinity values, where more negative scores indicate stronger ligand–protein interactions. Although the standard exhibits a marginally stronger binding affinity (-7.95 kcal/mol) compared to A1’s best green pose (-7.15 kcal/mol), the difference is slight enough to suggest that A1 is highly competitive. The right panel presents the RMSD values, with lower RMSD—ideally between 1.5 and 2.5 Å—indicating more stable binding conformations. Here, A1 (1.91 Å) shows a slightly better (lower) RMSD than the standard (2.11 Å), indicating that its binding pose is more consistently stable and well-aligned within the active site. Together, these metrics highlight that the green-highlighted A1 pose represents the optimal conformation among its three docking variants, making it a promising candidate for further development.

4. CONCLUSION

This study effectively synthesizes sulfadiazine-imine derivatives utilizing a microwave-assisted technique with quick reaction durations, high yields, and purity. Sulfadiazine's biological characteristics improved after imine synthesis using orsellinaldehyde and 2-hydroxy-5-methylbenzaldehyde. Compared to the original sulfadiazine, both derivatives, especially A1, were more effective against *Bacillus subtilis*, *Escherichia coli*, and *Streptococcus pneumoniae*. Larger inhibitory zones showed that imine modification increased membrane penetration and bacterial susceptibility. In addition, compounds A1 and A2 showed significant, dose-dependent anticancer action on MCF-7 breast cancer cells, with IC₅₀ values between 40 and 80 ppm. These results show that chemical derivatization of sulfadiazine might improve its antibacterial and anticancer capabilities, addressing antibiotic resistance and the need for novel anticancer drugs. Increased lipophilicity and biological target contact may explain the derivatives' higher effectiveness. In conclusion, microwave-assisted synthesis is a powerful and environmentally friendly method for generating new sulfadiazine derivatives with therapeutic promise, promoting structural optimization and preclinical assessment for biomedical applications.

REFERENCES

- Alani, B. G., Salim, K. S., Mahdi, A. S., & Al-Temimi, A. A. (2024). Sulfonamide derivatives: Synthesis and applications. *Int. J. Front. Chem. Pharm. Res*, 4, 1-15.
- Ali, Z. H., Jber, N. R., & Abbas, A. K. (2023). Synthesis and characterization of new 1, 3-oxazepine compounds from P-Phenylenediamine as insecticide (Aphidoidea). *AIP Conference Proceedings*,
- Brüssow, H. (2024). The antibiotic resistance crisis and the development of new antibiotics. *Microbial Biotechnology*, 17(7), e14510.
- Chen, Y., Wang, Y., Wang, J., Zhou, Z., Cao, S., & Zhang, J. (2023). Strategies of targeting CK2 in drug discovery: challenges, opportunities, and emerging prospects. *Journal of Medicinal Chemistry*, 66(4), 2257-2281.
- Chinemerem Nwobodo, D., Ugwu, M. C., Oliseloke Anie, C., Al-Ouqaili, M. T., Chinedu Ikem, J., Victor Chigozie, U., & Saki, M. (2022). Antibiotic resistance: The challenges and some emerging strategies for tackling a global menace. *Journal of clinical laboratory analysis*, 36(9), e24655.
- Christensen, S. B. (2021). Drugs that changed society: History and current status of the early antibiotics: Salvarsan, sulfonamides, and β -lactams. *Molecules*, 26(19), 6057.
- Coanda, M., Limban, C., Draghici, C., Ciobanu, A.-M., Grigore, G. A., Popa, M., Stan, M., Larion, C., Avram, S., & Mares, C. (2024). Current Perspectives on Biological

Screening of Newly Synthetised Sulfanilamide Schiff Bases as Promising Antibacterial and Antibiofilm Agents. *Pharmaceuticals*, 17(4), 405.

- Elangovan, N., Sowrirajan, S., Arumugam, N., Almansour, A. I., Altaf, M., & Mahalingam, S. M. (2024). Synthesis, vibrational analysis, absorption and emission spectral studies, topology and molecular docking studies on sulfadiazine derivative. *ChemistrySelect*, 9(10), e202303582.
- Elangovan, N., Thomas, R., Sowrirajan, S., & Irfan, A. (2021). Synthesis, spectral and quantum mechanical studies and molecular docking studies of Schiff base (E) 2-hydroxy-5-(((4-(N-pyrimidin-2-yl) sulfamoyl) phenyl) imino) methyl benzoic acid from 5-formyl salicylic acid and sulfadiazine. *Journal of the Indian Chemical Society*, 98(10), 100144.
- Elkanzi, N. A., Alsirhani, A. M., Ali, A. M., Abdou, A., & Alali, I. (2025). Design, characterization, antioxidant activity, and molecular docking study of sulfadiazine derivative-based Ni (II) and Cu (II) complexes. *Journal of Molecular Liquids*, 126937.
- Gomaa, M., Gad, W., Hussein, D., Pottoo, F. H., Tawfeeq, N., Alturki, M., Alfahad, D., Alanazi, R., Salama, I., & Aziz, M. (2024). Sulfadiazine exerts potential anticancer effect in HepG2 and MCF7 cells by inhibiting TNF α , IL1b, COX-1, COX-2, 5-LOX gene expression: evidence from in vitro and computational studies. *Pharmaceuticals*, 17(2), 189.
- Hassan, S. A., Aziz, D. M., Abdullah, M. N., Bhat, A. R., Dongre, R. S., Ahmed, S., Rahiman, A. K., Hadda, T. B., Berredjem, M., & Jamalis, J. (2023). Design and synthesis of oxazepine derivatives from sulfonamide Schiff bases as antimicrobial and antioxidant agents with low cytotoxicity and hemolytic prospective. *Journal of Molecular Structure*, 1292, 136121.
- Hassan, S. A., Aziz, D. M., Kader, D. A., Rasul, S. M., Muhamad, M. A., & Muhammedamin, A. A. (2024). Design, synthesis, and computational analysis (molecular docking, DFT, MEP, RDG, ELF) of diazepine and oxazepine sulfonamides: Biological evaluation for in vitro and in vivo anti-inflammatory, antimicrobial, and cytotoxicity predictions. *Molecular Diversity*, 1-23.
- Jawad, A. A., Jber, N. R., Rasool, B. S., & Abbas, A. K. (2023). Tetrazole derivatives and role of tetrazole in medicinal chemistry: An article review. *Al-Nahrain Journal of Science*, 26(1), 1-7.
- Mohammed, T. T., Obaid, A. H., Hammeed, G. F., & Abbas, A. K. (2024). Modification of Sulfadiazine Antibacterial to Promising Anticancer Schiff Base Derivatives: Synthesis and in Vitro Studies. *The International Science of Health Journal*, 2(3), 01-10.
- Oreshko, V. V., Kovaleva, K. S., Mordvinova, E. D., Yarovaya, O. I., Gatilov, Y. V., Shcherbakov, D. N., Bormotov, N. I., Serova, O. A., Shishkina, L. N., & Salakhutdinov, N. F. (2022). Synthesis and antiviral properties of camphor-derived iminothiazolidine-4-ones and 2, 3-dihydrothiazoles. *Molecules*, 27(15), 4761.
- Ovung, A., & Bhattacharyya, J. (2021). Sulfonamide drugs: Structure, antibacterial property, toxicity, and biophysical interactions. *Biophysical reviews*, 13(2), 259-272.

- Rohilla, S., & Sharma, D. (2023). Sulfonamides, quinolones, antiseptics, and disinfectants. In *Medicinal Chemistry of Chemotherapeutic Agents* (pp. 21-63). Elsevier.
- Soliman, A.-Q. S., Abdel-Latif, S. A., Abdel-Khalik, S., Abbas, S. M., & Ahmed, O. M. (2024). Design, synthesis, structural characterization, molecular docking, antibacterial, anticancer activities, and density functional theory calculations of novel MnII, CoII, NiII, and CuII complexes based on pyrazolone-sulfadiazine azo-dye ligand. *Journal of Molecular Structure*, 1318, 139402.
- Srinithi, S., Arumugam, B., Chen, S.-M., Annamalai, S., & Ramaraj, S. K. (2023). Synthesis and characterization of pyrochlore-type lanthanum cerate nanoparticles: Electrochemical determination of antibiotic drug sulfadiazine in biological and environmental samples. *Materials Chemistry and Physics*, 296, 127244.
- Zheng, H., Zhang, Y., Li, S., Feng, X., Wu, Q., Leong, Y. K., & Chang, J.-S. (2023). Antibiotic sulfadiazine degradation by persulfate oxidation: Intermediates dependence of ecotoxicity and the induction of antibiotic resistance genes. *Bioresource technology*, 368, 128306.